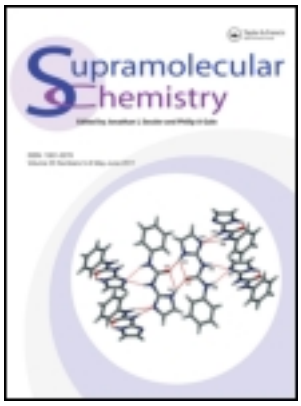

Supramolecular Chemistry
Publication details, including instructions for authors and subscription information:
http://www.tandfonline.com/loi/gsch20

Metal ion complexation in acetonitrile by cone, di-ionised calix[4]arene-1,2-crown ethers with two pendant dansyl fluorophores

Ümmühan Ocak [a], Miraç Ocak [a], Chuqiao Tu [b] & Richard A. Bartsch [b]

[a] Department of Chemistry, Faculty of Arts and Sciences, Karadeniz Technical University, 61080, Trabzon, Turkey

[b] Department of Chemistry and Biochemistry, Texas Tech University, Lubbock, TX, 79409, USA

Available online: 31 Oct 2011

To cite this article: Ümmühan Ocak, Miraç Ocak, Chuqiao Tu & Richard A. Bartsch (2011): Metal ion complexation in acetonitrile by cone, di-ionised calix[4]arene-1,2-crown ethers with two pendant dansyl fluorophores, Supramolecular Chemistry, 23:11, 743-752

To link to this article: http://dx.doi.org/10.1080/10610278.2011.626039

Supramolecular Chemistry
Vol. 23, No. 11, November 2011, 743–752

Metal ion complexation in acetonitrile by cone, di-ionised calix[4]arene-1,2-crown ethers with two pendant dansyl fluorophores

Ümmühan Ocak[a]*, Miraç Ocak[a], Chuqiao Tu[b] and Richard A. Bartsch[b]

[a]*Department of Chemistry, Faculty of Arts and Sciences, Karadeniz Technical University, 61080 Trabzon, Turkey;* [b]*Department of Chemistry and Biochemistry, Texas Tech University, Lubbock, TX 79409, USA*

(*Received 1 October 2010; final version received 12 September 2011*)

Four cone calix[4]arene-1,2-crown ethers each with two ionisable side arms containing dansyl groups are synthesised. The crown ether ring on the lower rim is varied from crown-4 to crown-5 with hydrogen or *tert*-butyl groups on the para position of the upper rim. Di(tetramethylammonium) salts of the di-ionised ligands are utilised for spectrofluorimetric titration experiments in MeCN. The influence of alkali metal, alkaline earth metal and selected transition and heavy metal (Co^{2+}, Fe^{2+}, Hg^{2+}, Mn^{2+}, Pb^{2+}, Zn^{2+} and Fe^{3+}) cations on the spectroscopic properties of the two dansyl groups linked to the lower rim of the conformationally locked, di-ionised calix[4]arene-1,2-crown ether frameworks is investigated by emission spectrophotometry. All of the metal cations induce red shifts in the emission spectra of the di-ionised ligands. The metal cations produce enhancement or quenching of the fluorescence emissions. Changes in the fluorescence emission as a function of the metal cation identity, the lower rim crown ether ring size and the absence or presence of upper rim *tert*-butyl groups are investigated.

Keywords: calixarene-crown ether ligand; fluorescence spectroscopy; stability constant; metal ion complexation

1. Introduction

Calix[n]arenes are an important class of macrocyclic ligands for metal ions (*1–3*). The attachment of substituents to the upper and/or lower rims of the macrocyclic scaffolds may produce metal ion complexing agents with high selectivities (*4–9*). Also, cation–π interactions by the benzene rings of the calixarene scaffold may facilitate complexation of soft metal cations (*10–12*).

Calix[4]arene compounds may be obtained as conformationally mobile ligands or as conformationally restricted isomers (cone, partial-cone, 1,2-alternate and 1,3-alternate), depending upon the identity of groups attached to the macrocyclic framework (*3*). In earlier work (*13–17*), we prepared novel calix[4]arene compounds with two dansyl group-containing side arms (—$OCH_2C(O)NHSO_2C_6H_4$—4—$N(CH_3)_2$) and two methoxy groups attached to the macrocyclic ring. After conversion to di-ionised tetramethylammonium salts, interactions of the resultant ligands with alkali metal, alkaline earth and selected transition and heavy metal cations in MeCN were probed by fluorescence spectroscopy. Fluorescence emission was almost completely quenched in the presence of Fe^{3+}, Hg^{2+} and Pb^{2+}. Due to the presence of the two methoxy groups on the macrocyclic scaffold, these calix[4]arene-based ligands were conformationally mobile. To probe the influence of fixing the conformation, calix[4]arene-crown ether analogues were envisioned in which the methoxy groups are replaced by a polyether unit attached on both ends to the macrocyclic scaffold.

We now report the synthesis of cone compounds **1–4** (Scheme 1) in which fluorogenic dansyl groups are incorporated into two acidic side arms on the lower rim. Systematic structural variations in this conformationally restricted series include (i) a change from a crown ether ring with four oxygens (in **1** and **3**) on the lower rim to one with five oxygens (in **2** and **4**) and (ii) the absence (in **1** and **2**) or presence (in **3** and **4**) of *tert*-butyl groups on the upper rim in positions para to the attachments sites of the phenolic oxygens. The effects of these structural variations on the complex stability of di(tetramethylammonium) salts of the di-ionisable ligands **1–4** with a variety of metal cations are assessed by spectrofluorometric titrations in MeCN. Complex stability constants and complex compositions for Hg^{2+}, Pb^{2+} and Fe^{3+} with the four di-ionised ligands are determined.

2. Experimental

2.1 General

^{1}H NMR spectra were measured in $CDCl_3$ at 500 MHz with a Varian Unity INOVA spectrometer. IR spectra were recorded with a Perkin-Elmer model 1600 FT-IR

*Corresponding author. Email: uocak@ktu.edu.tr

ISSN 1061-0278 print/ISSN 1029-0478 online

http://dx.doi.org/10.1080/10610278.2011.626039
http://www.tandfonline.com

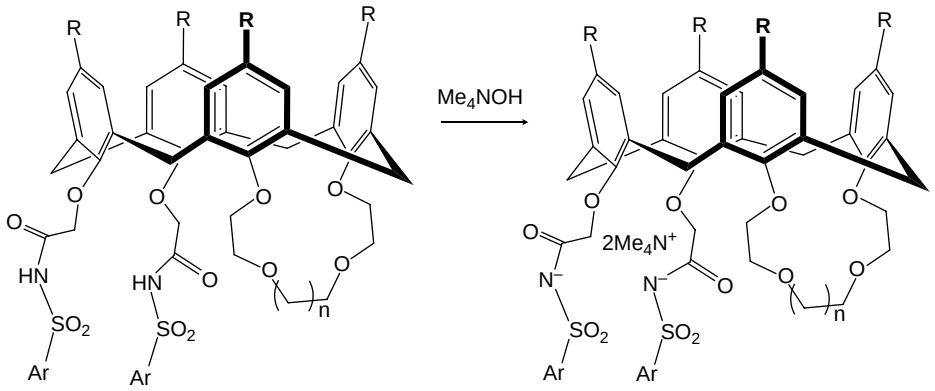

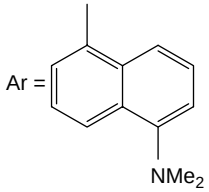

	R	n	
1	H	1	**C4**
2	H	2	**C5**
3	t–Bu	1	**TBC 4**
4	t–Bu	2	**TBC 5**

Scheme 1. Structures of ionophores **1**–**4** and their di-ionised tetramethylammonium salts.

spectrophotometer. Absorption spectra were recorded on a Shimadzu model 2401PC UV-visible spectrophotometer. Fluorescence spectra were obtained on a SLM Aminco 8000C photon counting spectrofluorometer equipped with a 450-W ozone-free xenon lamp as the light source. Combustion analysis was carried out at Desert Analytics Laboratory (now Columbia Analytical Services) in Tucson, Arizona.

Silica gel with a pore diameter ~4 nm was obtained from Acros Organics (Pittsburgh, PA, USA). MeCN from EM (spectrometric grade) was utilised as the solvent for the fluorescence measurements. Alkali metal and earth alkaline metal perchlorates from Acros were of the highest quality available and were vacuum dried over the silica gel before use. Other metal perchlorates were available from previous studies (*15–18*). Dicarboxylic acid precursors to didansyl calix[4]arene-1,2-crown compounds **1**–**4** were prepared by reported procedures (*19–22*). Combustion analysis results for compounds **1**–**4** indicated partial solvates with dichloromethane. Confirming peaks for dichloromethane at $\delta = 5.32$ were observed in their ^{1}H NMR spectra.

2.2 Fluorescence measurements

Fluorescence spectra of the di-ionised ligands (2.58×10^{-5} M) in MeCN solutions containing 50 molar equiv. of the appropriate metal perchlorate salt were measured using a 1-cm quartz cell. The excitation wavelength was 326 nm for ligands **C4** and **C5**. The excitation wavelength was 327 nm for ligands **TBC4** and **TBC5**. Fluorescence emission spectra were recorded in the range of 400–600 nm with a slit width of 1.0 nm.

The stoichiometries of the complexes and their stability constants were determined according to the literature procedure (*23*).

2.3 Ligand synthesis

2.3.1 General procedure for the preparation of di-ionisable calix[4]arene-1,2-crown ethers *1–4*

A solution of dry benzene (40 ml), the appropriate calix[4]arene-1,2-crown ether di(carboxylic acid) (1.0 equiv.) and oxalyl chloride (16.0 equiv.) was stirred at 50–55°C for 12 h. The benzene was evaporated *in vacuo* to give the corresponding di(acid chloride), which was used directly in the next step. In a three-necked flask under nitrogen, a mixture of NaH (10.0 equiv.) in THF (30 ml) was stirred at room temperature for 1.5 h followed by dropwise addition of a solution of dansylamide (2.2 equiv.) in THF (10 ml) over a 10-min period. The mixture was stirred at room temperature for 24 h after which H_2O (10 ml) was added and stirring was continued for 0.5 h. The THF was evaporated *in vacuo* and CH_2Cl_2 was added to the residue. The organic layer was separated, dried over $MgSO_4$ and evaporated *in vacuo*. The residue was chromatographed on silica gel. The eluted product was dissolved in CH_2Cl_2, and the solution was shaken with 6 N HCl. The organic layer was separated, dried over $MgSO_4$ and evaporated *in vacuo* to give the solid product.

*2.3.1.1 25,26-Bis(N-dansylsulphonyl carbamoylmethoxy)calix[4]arene-1,2-crown-4 (**1**) in the cone conformation*. Using hexanes–EtOAc (1:4) as eluent, 42% of yellow solid was obtained with mp 208–210°C. IR (deposit from CH_2Cl_2 on a NaCl plate): 3250 (N—H); 1714 (C = O); 1349, 1144 (SO_2) cm^{-1}.^{1}H NMR: δ 10.91 (br s, 1H), 8.67 (d, $J = 7.3$ Hz, 2H), 8.62 (t, $J = 7.6$ Hz, 2H), 8.42 (d, $J = 7.9$ Hz, 1H), 7.59 (t, $J = 7.9$ Hz, 2H), 7.48 (t, $J = 7.9$ Hz, 2H), 7.14 (d, $J = 6.7$ Hz, 1H), 7.04 (d, $J = 6.0$ Hz, 1H), 6.97 (d, $J = 7.2$ Hz, 1H), 6.94 (d, $J = 7.1$ Hz, 1H), 6.84 (d, $J = 6.0$ Hz, 1H), 6.76 (t, $J = 7.6$ Hz, 1H), 6.72–6.11 (m, 9H), 5.02 (d, $J = 14.5$ Hz, 2H), 4.88 (d, $J = 13.2$ Hz, 1H), 4.52 (d, $J = 13.3$ Hz, 1H), 4.29 (d, $J = 14.6$ Hz, 2H), 4.46–4.22 (br s, 2H), 4.19 (d, $J = 13.9$ Hz, 2H), 4.12–3.54 (m, 9H), 3.45 (br s, 2H), 3.33 (d, $J = 12.0$ Hz), 3.18 (d, $J = 14.0$ Hz, 2H), 3.14 (d, $J = 13.6$ Hz, 1H), 2.99 (s, 6H), 2.87 (s, 6H), 2.70 (d, $J = 13.7$ Hz, 1H). ^{13}C NMR: δ 168.7, 156.2, 155.9, 152.9, 135.2, 135.0, 134.8, 134.6, 133.9, 133.5, 133.3, 132.8, 132.7, 131.6, 129.9, 129.7, 129.5, 129.1, 128.8, 128.5, 128.4, 125.9, 125.8, 123.6, 122.7, 122.6, 118.8, 115.3, 74.0, 73.7, 70.7.70.2, 45.5, 31.7, 31.6, 29.5. Anal. Calcd for $C_{62}H_{62}O_{12}N_4S_2 \cdot 0.3CH_2Cl_2$: C, 65.36; H, 5.51; N, 4.82. Found: C, 65.60; H, 5.52; N, 4.74.

*2.3.1.2 25,26-Bis(N-dansylsulphonyl carbamoylmethoxy)calix[4]arene-1,2-crown-5 (**2**) in the cone conformation*. Using CH_2Cl_2–MeOH (39:1) as eluent, 57% of yellow solid was obtained with mp 208–210°C. IR (deposit from CH_2Cl_2 on a NaCl plate): 3209 (N—H), 1720 (C = O), 1349, 1141 (SO_2) cm^{-1}.^{1}H NMR: δ 10.81 (br s, 2H), 8.83 (br s, 2H), 8.70–8.38 (m, 4H), 7.61 (t, $J = 7.4$ Hz, 2H), 7.51 (br s, 2H), 7.38 (br s, 2H), 6.76–6.24 (m, 12H), 4.89 (d, $J = 14.8$ Hz, 2H), 4.60 (d, $J = 13.7$ Hz, 1H), 4.48 (d, $J = 16.0$ Hz, 2H), 4.42 (d, $J = 13.2$ Hz, 1H), 4.27 (d, $J = 13.8$ Hz, 2H), 4.03 (d, $J = 5.7$ Hz, 6H), 3.88 (br s, 4H), 3.84–3.52 (m, 6H), 3.14 (d, $J = 13.7$ Hz, 1H), 3.14 (d, $J = 13.7$ Hz, 2H), 3.07 (s, 12H), 2.93 (d, $J = 13.9$ Hz, 1H). ^{13}C NMR: δ 168.6, 155.9, 155.6, 135.0, 134.4, 134.0, 133.1, 132.5, 129.5, 129.0, 128.4, 128.1, 122.9, 122.7, 73.9, 73.4, 70.4, 69.8, 46.2, 31.8, 31.2, 30.6. Anal. Calcd for $C_{64}H_{66}O_{13}N_4S_2 \cdot 0.6CH_2Cl_2$:C, 63.90; H, 5.58; N, 4.61. Found: C, 63.92; H, 5.56; N, 4.62.

*2.3.1.3 5,11,17,23-Tetrakis(1,1-dimethylethyl)-25,26-bis(N-dansylsulphonyl carbamoyl-methoxy)calix[4]arene-1,2-crown-4 (**3**) in the cone conformation*. With CH_2Cl_2–MeOH (19:1) as eluent, 76% of yellow solid was obtained with mp 228–230°C. IR (deposit from CH_2Cl_2 on a NaCl plate): 3300–2400 (N—H), 1721 (C = O), 1347, 1145 (SO_2) cm^{-1}.^{1}H NMR: δ 11.07 (br s, 2H), 9.32–8.34 (m, 6H), 7.75 (s, 2H), 7.66–7.35 (m, 4H), 7.10 (m, 8H), 5.05 (d, $J = 10.7$ Hz, 2H), 4.67 (d, $J = 12.4$ Hz, 1H), 4.29 (d, $J = 12.1$ Hz, 1H), 4.17 (d, $J = 12.1$ Hz, 2H), 4.10–3.64 (m, 10H), 3.53 (s, 2H), 3.24 (d, $J = 11.1$ Hz, 1H), 3.14 (d, $J = 13.2$ Hz, 2H), 3.10 (d, $J = 12.3$ Hz, 1H), 2.96 (s, 12H), 1.17–0.93 (m, 36H). ^{13}C NMR: δ 169.0, 158.9, 153.1, 150.4, 147.8, 147.5, 145.0, 144.9, 134.36,133.8, 132.8, 132.5, 131.9, 130.8, 129.6, 128.9, 128.4, 126.1, 125.8, 125.7, 125.6, 125.3, 125.2, 125.0, 124.1, 74.6, 73.6, 73.4, 70.5, 69.2, 68.4, 67.4, 45.8, 34.0, 33.8, 33.7, 31.7, 31.4, 31.2, 29.9, 29.1. Anal. Calcd for $C_{78}H_{94}O_{12}S_2N_4 \cdot 0.4CH_2Cl_2$: C, 68.35; H, 69.4; N, 4.07. Found: 68.15; H, 7.16; N, 3.73.

*2.3.1.4 5,11,17,23-Tetrakis(1,1-dimethylethyl)-25,26-bis(N-dansylsulphonyl carbamoyl-methoxy)calix[4]arene-1,2-crown-5 (**4**) in the cone conformation*. With hexanes–EtOAc (1:3) as eluent, 41% of yellow solid was obtained with a mp 178–180°C. IR (deposit from CH_2Cl_2 on a NaCl plate): 3245 (N—H), 1722 (C = O), 1362, 1144 (SO_2) cm^{-1}.^{1}H NMR: δ 10.64 (s, 2H), 8.60 (dd, $J = 7.0$, 1.0 Hz, 2H), 8.54 (d, $J = 8.4$ Hz, 2H), 8.39 (d, $J = 8.5$ Hz, 2H), 7.54 (dd, $J = 9.0$ Hz, 2H), 7.50 (dd, $J = 8.0$ Hz, 2H), 7.11 (d, $J = 7.4$ Hz, 2H), 6.78 (s, 2H), 6.66 (s, 4H), 4.85 (d, $J = 13.6$ Hz, 2H), 4.80 (d, $J = 12.7$ Hz, 1H), 4.54 (d, $J = 15.6$ Hz, 2H), 4.30 (d, $J = 12.3$ Hz, 2H), 4.29 (d, $J = 12.9$ Hz, 2H), 4.21–4.04 (m, 8H), 4.04–3.73 (m, 8H), 3.14 (d, $J = 12.4$ Hz, 1H), 3.08 (d, $J = 12.9$ Hz, 1H), 3.01 (d, $J = 12.9$ Hz, 1H), 2.86 (s, 12H), 1.05 (s, 18H), 1.01 (s, 18H). ^{13}C NMR: δ 169.1, 153.2, 152.9, 151.9, 145.2, 144.9, 133.8, 133.4, 133.3, 132.3, 131.7, 131.4, 129.6, 125.5, 125.4, 125.2, 125.1, 123.4, 118.6, 115.0, 74.0, 73.6, 70.43, 69.8, 69.2, 45.4, 33.8, 33.7, 32.6, 31.4, 31.3, 31.1,31.0. Anal. Calcd for $C_{80}H_{98}O_{13}S_2N_4 \cdot 0.5CH_2Cl_2$: C, 67.60; H, 6.98; N, 3.92. Found: C, 67.68; H, 6.82; N, 3.89.

2.3.2 Preparation of di(tetramethylammonium) salts of the di-ionised ligands

Di(tetramethylammonium) salts of ligands (**C4**, **C5**, **TBC4** and **TBC5**) were prepared from ligands **1**–**4**, respectively, according to the published procedure (*15*).

3. Results and discussion

3.1 Ligand synthesis

Precursors of ligands **1**–**4** with two lower rim oxyacetic acid side arms are the reported compounds (*19*–*22*). The appropriate calix[4]arene-1,2-crown ether di(carboxylic acid) was refluxed with oxalyl chloride in C_6H_6 to provide the corresponding di(acid chloride). Addition of the crude di(acid chloride) to a mixture of NaH and dansylamide (1-dimethylamino-naphthalene-5-sulphonamide) in THF at room temperature produced ligands **1**–**4** in modest yields (41–76%). Structures of new compounds **1**–**4** were

verified by their ^{1}H NMR, ^{13}C NMR and IR spectra and by combustion analysis.

Ligands **1**–**4** were converted into their di(tetramethylammonium) salts **C4**, **C5**, **TBC4** and **TBC5**, respectively, by a reported method (*15*).

3.2 *Fluorescence spectra*

Fluorescence spectroscopy was utilised to probe the interactions of metal cations with the di-ionised ligands **C4** and **C5** (without *tert*-butyl groups on the upper rim) and **TBC4** and **TBC5** (with *tert*-butyl groups on the upper rim) in MeCN. Changes in the emission spectrum of a di-ionised ligand in the presence of a large excess (50 equiv.) of alkali metal, alkaline earth metal and selected transition and heavy metal (Co^{2+}, Fe^{2+}, Hg^{2+}, Mn^{2+}, Pb^{2+}, Zn^{2+} and Fe^{3+}) perchlorates in MeCN were measured (*15*–*18*).

When excited at 326 nm, ligands **C4** and **C5** gave emission bands with maxima at 483 and 479 nm, respectively (Figure 1). The effects of 17 metal cation species on the fluorescence spectrum of **C4** in MeCN are presented in Figure 1(a). As can be seen, red shifts were observed for all of the metal cations. The red shifts may be explained as resulting from photoinduced charge transfer. The dansyl fluorophore includes an electron-donating group (dimethylammonio) conjugated to an electron-withdrawing unit (carbonyl group). The electron-donating character of the former increases when a metal ion interacts with the carbonyl group. Thus, metal ion binding results in enhanced photoinduced charge transfer from the dimethylammonio group to the carboxyl group. Consequently, a red shift is observed.

In the presence of alkali metal cations, the emission band intensity for **C4** increased substantially, except for

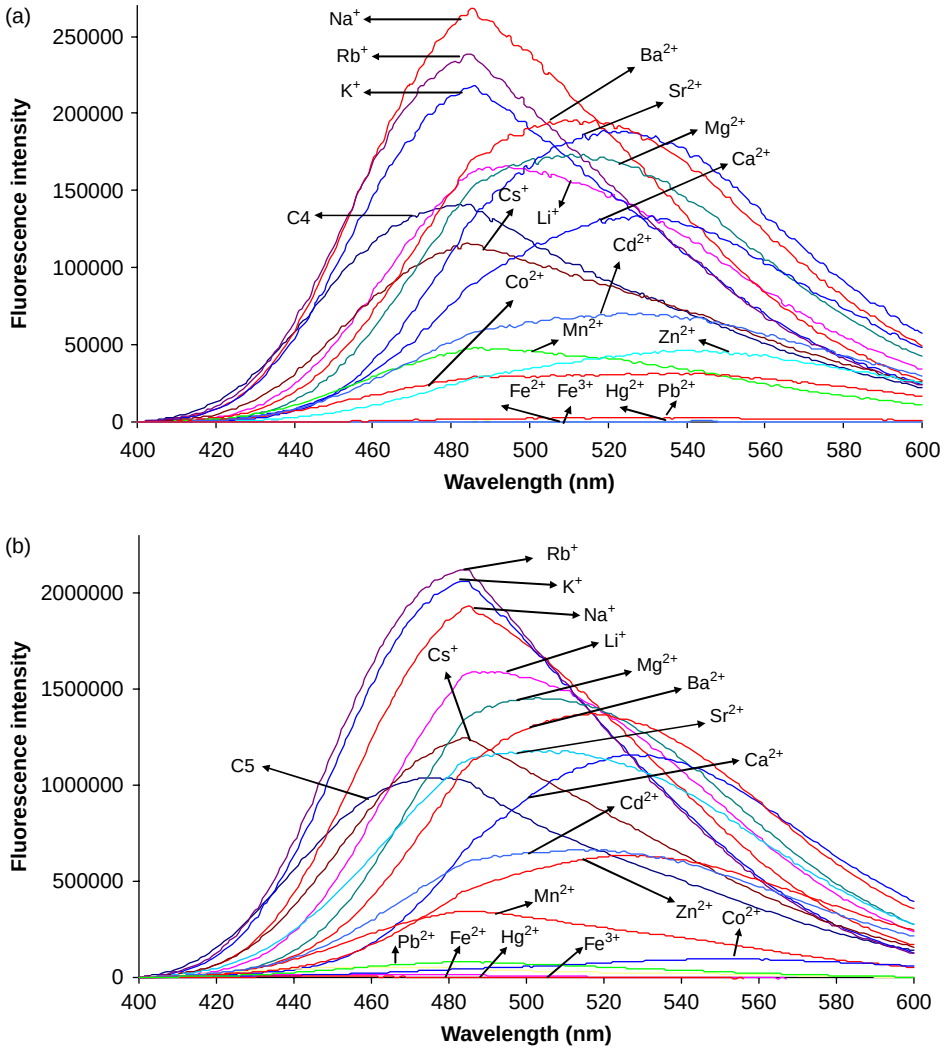

Figure 1. Effect of metal cations on the fluorescence spectra of (a) **C4** and (b) **C5** in MeCN. [L] = 2.58×10^{-5} M; [monovalent metal perchlorate] = 2.58×10^{-3} M; [divalent metal perchlorate] = 1.29×10^{-3} M; [trivalent metal perchlorate] = 8.60×10^{-4} M.

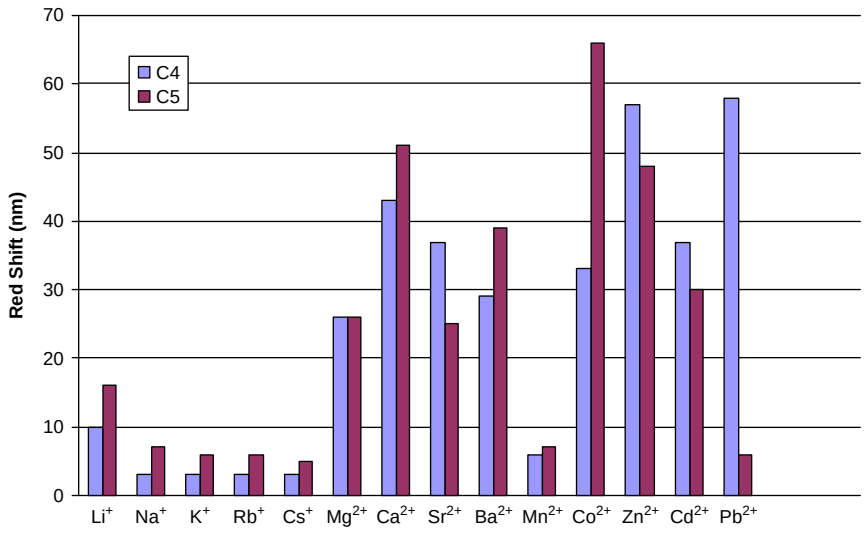

Figure 2. Bar graph of the red shift of the fluorescence emission observed at the wavelength of maximum emission for different metal cations with di-ionised ligands **C4** and **C5**.

Cs^+, which gave quenching. This result suggests a different fluorescence mechanism with Cs^+ from that for the other alkali metal cations. The alkaline earth metal cations, except for Ca^{2+}, caused increases in the fluorescence intensity of **C4**. However, the enhancements were greater for the alkali metal cations than for the alkaline earth metal cations. There was strong quenching of the fluorescence emission with the transition metal cations of Fe^{3+}, Fe^{2+}, Hg^{2+} and Pb^{2+}. Interaction of these cations may cause the fluorescence to be quenched via electron or energy transfer to the metal ion causing rapid non-radiative decay.

Figure 1(b) shows the effects of 17 metal cation species on the fluorescence spectrum of **C5** in MeCN. Once again, red shifts are noted for all of the metal ions. The alkali and alkaline earth metal cations all produced fluorescence enhancements. Noteworthy are the dramatic fluorescence enhancements in the presence of Na^+, K^+ and Rb^+. For Cs^+ and Ca^{2+}, the fluorescence enhancement was small.

The magnitudes of the red shifts in the fluorescence emissions for **C4** and **C5** are compared graphically in Figure 2 (no red shift data are shown for Fe^{2+}, Fe^{3+} and Hg^{2+} due to the very strong quenching by these metal

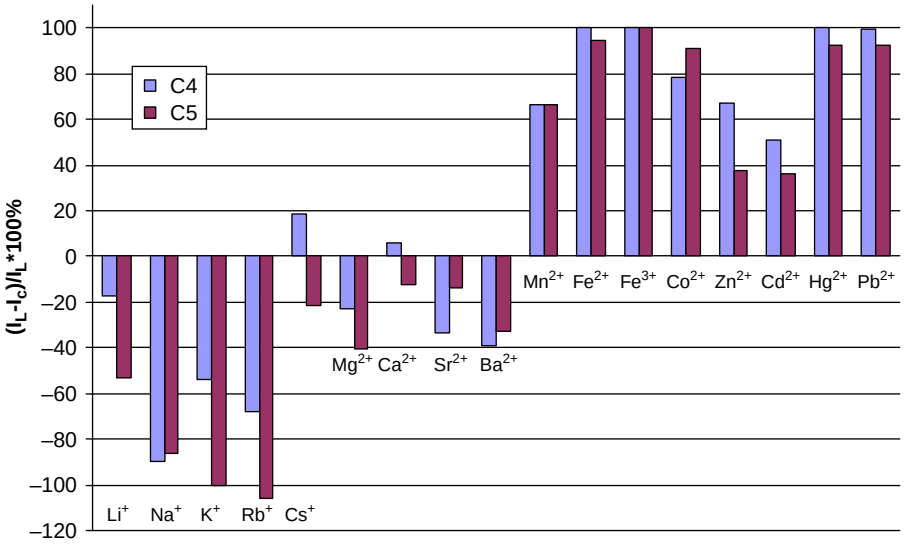

Figure 3. Bar graph of quenching efficiency for different metal cations observed at the wavelength of maximum emission for the di-ionised ligands **C4** and **C5**.

cations). Increasing the crown ether cavity size from crown-4 to crown-5 gave enhancements in the red shifts for the alkali metal cations with the largest red shift observed for Li^+. For the alkaline earth metal cations, Ca^{2+} gave the largest red shifts for both ligands. The alkaline earth metal cations produced larger red shifts than did the alkali metal cations. Among the transition metal cations and Pb^{2+}, the largest red shift was observed for Co^{2+} with **C5**. The largest effect of changing the crown ether ring size on the red shifts was observed for Pb^{2+}. Thus, **C5** gave a red shift of 6 nm upon interaction with this cation. However, a red shift of 58 nm was observed for Pb^{2+} and **C4**. For Cd^{2+} and Zn^{2+}, decreases in the red shifts were observed with an increase in the crown ether ring size. Conversely, increases in the red shifts were observed with the enhancement of the crown ether cavity size for Mn^{2+} and Co^{2+}.

Figure 3 shows the fluorescence intensity efficiency at maximum emission wavelength for the ionised ligands **C4** and **C5** in the presence of the metal cations. Pronounced fluorescence enhancement was observed with the alkali metal cations for both ligands, except for Cs^+ with **C4**. The enhancements were greatest for **C5** with K^+ and Rb^+. For Cs^+, the fluorescence mechanism must be different for the two ligands. With **C4**, the dansyl fluorescence was quenched by Cs^+. However, a fluorescence enhancement with Cs^+ was observed with **C5**. Among the alkaline earth metal cations, Ca^{2+} showed a similar effect. The effect of Sr^{2+} and Ba^{2+} was opposite to that of Mg^{2+} in relation to the crown ether cavity size. Thus, Mg^{2+} gave a greater fluorescence enhancement when the crown ether ring size was larger. However, Sr^{2+} and Ba^{2+} produced greater fluorescence enhancement when the crown ether ring size was reduced. All of the transition metal cations and Pb^{2+}

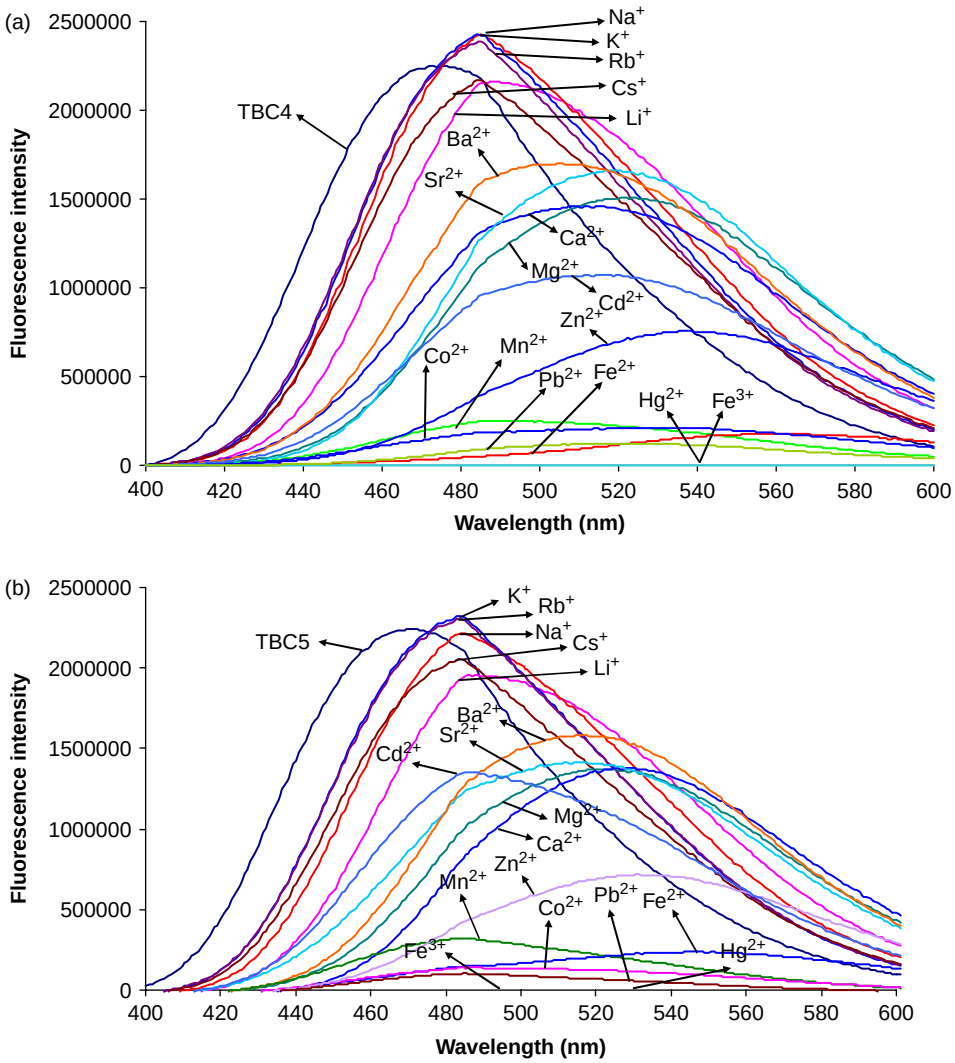

Figure 4. Effect of metal cations on the fluorescence spectra of (a) **TBC4** and (b) **TBC5** in MeCN. [L] = 2.58×10^{-5} M; [monovalent metal perchlorate] = 2.58×10^{-3} M; [divalent metal perchlorate] = 1.29×10^{-3} M; [trivalent metal perchlorate] = 8.60×10^{-4} M.

caused strong quenching in the fluorescence spectra for both **C4** and **C5**. The quenching was greater than 95% with Fe^{2+}, Fe^{3+}, Hg^{2+} and Pb^{2+}.

Di-ionised ligands **TBC4** and **TBC5** have the same structures as **C4** and **C5** except for the introduction of *tert*-butyl groups on their upper rims. When excited at 327 nm, **TBC4** and **TBC5** gave emission bands with maxima at 472 and 474 nm, respectively (Figure 4). Figure 4(a) shows the effects of 17 metal cation species on the fluorescence spectra of **TBC4** in MeCN. Red shifts were observed for all metal cation species. Na^+, K^+ and Rb^+ caused enhancements in the fluorescence intensity of **TBC4**, like those noted earlier for **C4**. Unlike **C4**, quenching was observed for alkaline earth metal cations. This result reveals that the *tert*-butyl groups play a role in the fluorescence mechanism in the case of alkaline earth metal cations. Transition metal cations produced quenching in the fluorescence intensity of **TBC4**. In particular, Fe^{3+} and Hg^{2+} gave greater than 99% quenching.

Figure 4(b) shows the effects of 17 metal cation species on the fluorescence spectrum of **TBC5**. Red shifts were noted for all metal cation species. K^+ and Rb^+ caused small fluorescence enhancements, and there was almost no change in the fluorescence intensity of **TBC5** in the presence of Na^+. Other alkali metal cations and the alkaline earth metal cations gave fluorescence quenching for **TBC5**. The quenching was stronger in the case of the alkaline earth metal cations. Strong quenching was observed for transition metal cations and Pb^{2+}.

The magnitudes of the red shifts in the fluorescence emissions for **TBC4** and **TBC5** are presented graphically in Figure 5. For alkali metal cations, there was no appreciable effect of changing the crown ether cavity size on the red shifts. Among the alkali metal cations, the largest red shifts were observed with Li^+ for both the ligands. The other alkali metal cations exhibited very similar red shifts for both the ligands. The alkaline earth metal cations gave larger red shifts for both the ligands than did the alkali metal cations. With Mg^{2+}, the red shifts for **TBC4** and **TBC5** were similar in magnitude. With Ca^{2+} and Ba^{2+}, the red shifts were appreciably larger with **TBC5** than with **TBC4**. On the other hand, the red shift diminished somewhat when the crown ether ring size was increased with Sr^{2+}. Similarly, smaller red shifts were obtained for all of the transition metal cations and Pb^{2+} in going from **TBC4** to **TBC5**. The largest red shifts of 75 and 80 nm were observed for Fe^{2+} with **TBC4** and **TBC5**, respectively. For Pb^{2+}, the red shift was larger than 50 nm for interaction with **TBC4**.

By comparing the data of Figures 2 and 5, the effect of introducing upper rim *tert*-butyl groups on the red shifts in the fluorescence emissions of ligands **C4** and **C5** may be deduced. For alkali metal cations, **TBC4** and **TBC5** with *tert*-butyl groups on the upper rim exhibited larger red shifts in the fluorescence spectra with respect to analogous ligands **C4** and **C5**. For alkaline earth metal cations, the introduction of *tert*-butyl groups had only relatively minor effects on the red shifts. For Co^{2+}, the red shifts were below 25 nm for **TBC4** and **TBC5**, while they were above 30 nm for **C4** and **C5**. For **TBC5**, the red shift in the presence of Co^{2+} was about 15 nm compared with about 65 nm for **C5**. This shows a detrimental effect of upper rim *tert*-butyl groups on the red shift for Co^{2+}.

Figure 6 presents the fluorescence intensity efficiency at maximum emission wavelength for ligands **TBC4** and **TBC5** upon addition of the metal cations. The effect of upper rim *tert*-butyl groups on the fluorescence response of the ligands upon interaction with alkali and alkaline earth metal cations may be deduced by comparing the data of Figures 3 and 6. As seen from Figure 6, the presence of

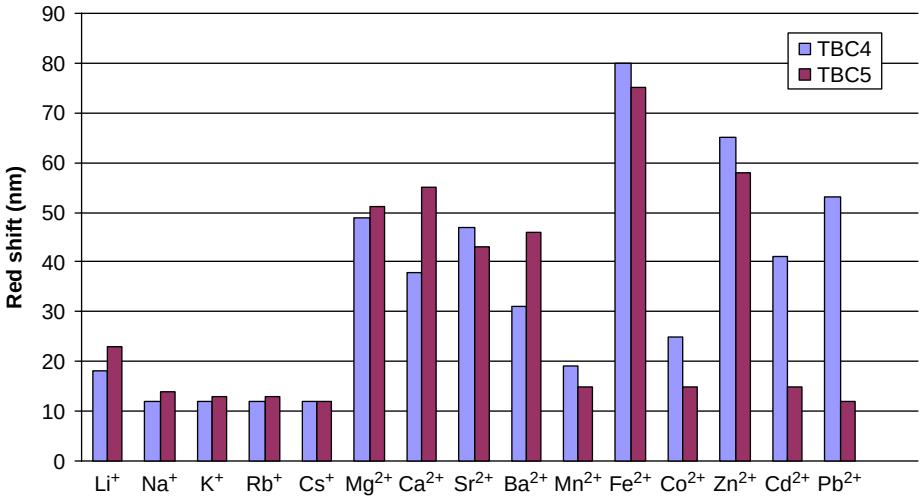

Figure 5. Bar graph of the red shift of the fluorescence emission observed at the wavelength of maximum emission for different metal cations with di-ionised ligands **TBC4** and **TBC5**.

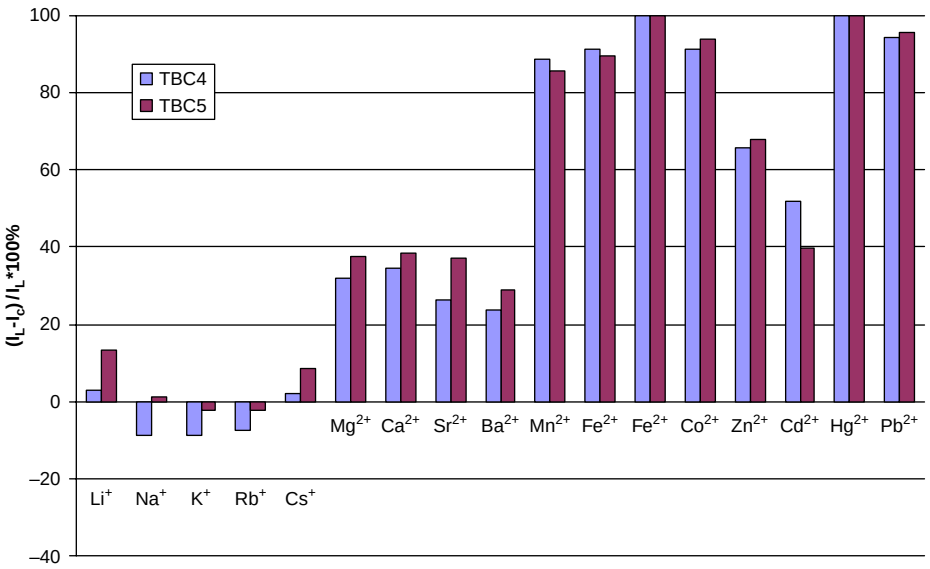

Figure 6. Bar graph of quenching efficiency for different metal cations observed at the wavelength of maximum emission for the di-ionised ligands **TBC4** and **TBC5**.

tert-butyl groups caused a little change in the fluorescence responses of ligands **TBC4** and **TBC5** to alkali metal cations. As mentioned previously, small changes in the red shifts were observed for these ligands in the presence of alkali metal cations. However, pronounced changes in the fluorescence responses were observed for alkali metal cations with **C4** and **C5** (Figure 3). Thus, the absence of *tert*-butyl groups favours stronger interactions with alkali metal cations. Another interesting result is the differing effect of alkaline earth metal cations for the fluorescence responses for the two series of ligands. As noted in Figure 6, all of the alkaline earth metal cations caused quenching of the fluorescence intensity for **TBC4** and **TBC5**, while the same cations generally produced fluorescence enhancements with **C4** and **C5** (Figure 3). Once again an effect of the presence of *tert*-butyl groups is evident. For the transition metal cations and Pb^{2+}, similar fluorescence responses were observed with upper rim *tert*-butyl groups absent (Figure 3) and present (Figure 6) in the di-ionisable calix[4]arene-crown ether ligands. This behaviour for the transition and heavy metal cations is in sharp contrast with that found for alkali and alkaline earth metal cations.

3.3 Determination of stability constants

Stability constants and stoichiometries for complexation of Hg^{2+}, Pb^{2+} and Fe^{3+} with the four di-ionised calix[4]arene-crown ether ligands were determined by fluorimetric titration. The titration experiments were performed by adding solutions with various concentrations of the metal perchlorate in MeCN to the solutions of the di-ionised ligand in MeCN. The ligand concentration was held constant at 2.58×10^{-5} M. Stoichiometries of the complexes and their stability constants were determined from changes in the fluorescence intensity as a function of the metal cation concentration. Successive decreases in emission with increases in the metal cation concentration eventually caused a complete disappearance of the emission in all of the fluorimetric titrations. The complex stability constant (β) was calculated using Valuer's method (*23*). Accordingly, the quantity $I_o/(I_o - I)$ was plotted versus [metal cation]$^{-1}$ with the stability constant given by the ratio of intercept/slope.

Figure 7 shows the fluorescence spectra of **TBC4** in MeCN with increasing concentrations of Hg^{2+}. The lower inset in Figure 7 is a plot of $I_o/(I_o - I)$ versus $[Hg^{2+}]^{-1}$ for the calculation of the stability constant. The upper inset in Figure 7 is a plot of the fluorescence intensity versus the ratio of [metal cation]/[ligand]. The observed break in the curve at [metal ion]/[ligand] = 1.0 provides strong evidence for the formation of a 1:1 complex. Similar plots were found for **TBC4** with Pb^{2+} and Fe^{3+}. Likewise, **C4** was observed to form 1:1 complexes with Hg^{2+}, Pb^{2+} and Fe^{3+}. Ligand **C4** forms more stable complexes than **TBC4** with Hg^{2+} and Pb^{2+}, but not with Fe^{3+} (Table 1). Ligand **C5** was found to form a stable complex only with Fe^{3+}. However, stable complexes were observed for **TBC5** with Hg^{2+} and Fe^{3+}. The largest stability constant (log β) of 5.27 was obtained with **C5** and Fe^{3+}.

3.4 Stern–Volmer analysis

Stern–Volmer analysis was utilised to probe the nature of the quenching process in the complexation of Fe^{3+}, Hg^{2+} and Pb^{2+} by ligand **C5**. Stern–Volmer plots are a useful

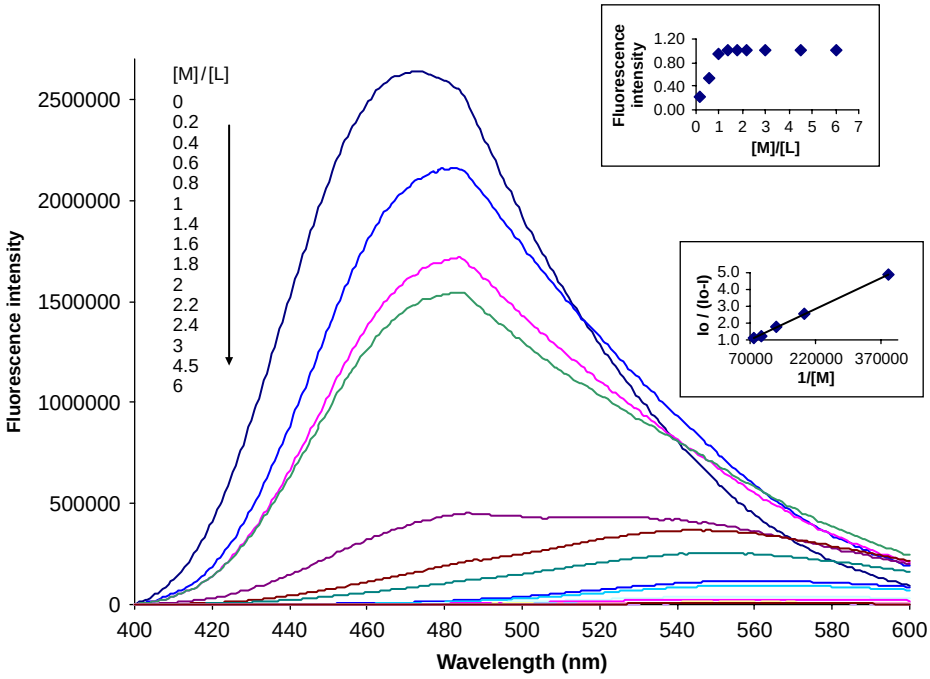

Figure 7. Fluorescence spectra ($\lambda_{exc} = 326$ nm and $\lambda_{em} = 472$) of **TBC4** in MeCN with increasing amounts of Hg^{2+} and [**TBC4**] $= 2.58 \times 10^{-5}$ M. See text for description of insets.

Table 1. Stability constants and complex stoichiometries for complexes of di-ionised calixarenes **C4**, **C5**, **TBC4** and **TBC5** with Hg^{2+}, Pb^{2+} and Fe^{3+} in MeCN.

	Stability constant (log β) cation			Complex stoichiometry (M:L) cation		
Di-ionised ligand	Fe^{3+}	Hg^{2+}	Pb^{2+}	Fe^{3+}	Hg^{2+}	Pb^{2+}
C4	4.33 ± 0.01	5.03 ± 0.03	4.39 ± 0.01	1:1	1:1	1:1
C5	5.27 ± 0.02	–	–	1:1	–	–
TBC4	4.81 ± 0.03	4.11 ± 0.02	4.16 ± 0.01	1:1	1:1	1:1
TBC5	4.91 ± 0.04	5.15 ± 0.03	–	1:1	1:1	–

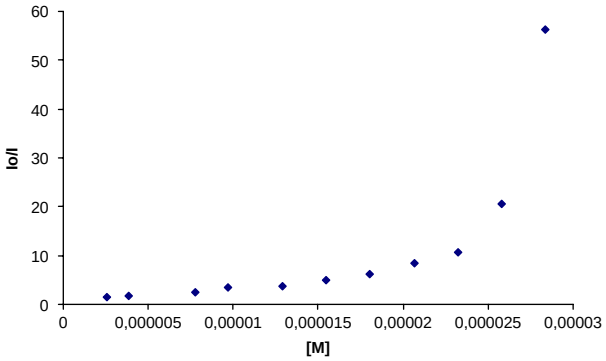

Figure 8. Stern–Volmer plot for the fluorescence quenching of **C5** by Fe^{3+} in MeCN.

method of presenting data on emission quenching (*24*, *25*). From the data, dynamic or static quenching processes can be determined. Plotting relative emission intensities (I_o/I) against quencher concentration [Q] for a static process should yield a linear Stern–Volmer plot. Expressed as Equation (1), the slope of the plot line yields K_{sv}, the static quenching constant.

$$\frac{I_o}{I} = 1 + K_{sv}[Q]. \quad (1)$$

Figure 8 shows the steady-state emission of Stern–Volmer analysis for Fe^{3+} with **C5**. Nonlinear behaviour with positive deviations from the typically linear Stern–Volmer analysis was observed. This result indicates that both static quenching and dynamic quenching are taking place.

4. Conclusions

This study probed the influence of variations of crown ether size and the introduction of upper rim para *tert*-butyl groups in calix[4]arene-1,2-crown ethers ligands having two ionised, dansyl-containing side arms on the lower rim upon their spectroscopic responses to metal ions. In the presence of excess Cs^{+} in MeCN, different fluorescence responses for calixarenes without *tert*-butyl groups on the upper rim (**C4** and **C5**) were observed when the crown ether ring on the lower rim was varied from crown-4 to crown-5. Fluorescence quenching appeared with the crown-4 compound, while an enhancement was observed in the case of the crown-5 analogue. A similar effect was observed for Ca^{2+} among the alkaline earth metal ions. These results demonstrate that the crown ether ring on the lower rim participates in the metal ion complexation. For all of the other alkali metal and alkaline earth metal cations, enhancements were observed on the fluorescence of the lower rim dansyl groups of **C4** and **C5**. On the other hand, fluorescence quenching was noted in the presence of transition metal ions and Pb^{2+}, in agreement with the results of previous studies conducted with di-ionisable calix[4]arene ligands. Fe^{3+}, Pb^{2+} and Hg^{2+} gave greater than 99% quenching of the dansyl fluorescence for both ligands. For the ligands with *tert*-butyl groups on the upper rim, different results were obtained with the alkali metal and alkaline earth metal cations. Alkaline earth metal cations produced fluorescence quenching similar to transition metal cations for ligands **TBC4** and **TBC5** with *tert*-butyl groups on the upper rim. These findings establish that the upper rim *tert*-butyl groups have a pronounced influence on varying the fluorescence responses of di-ionised calix[4]arene-1,2-crown ethers with the lower rim dansyl groups on the lower rim complexation of alkali and alkaline earth metal cations.

Acknowledgements

This work was supported by the Scientific and Technological Research Council of Turkey (TUBITAK). We also thank the Division of Chemical Sciences, Geosciences and Biosciences of the Office of Basic Energy Sciences of the US Department of Energy (Grant DE-FG02-90ER14416) for the support of this research.

References

(1) Gutsche, C.D. *Calixarenes*; Royal Society of Chemistry: Cambridge, 1989.
(2) Sliwa, W.; Deska, M. *ARKIVOC* **2008**, *i*, 87–127.
(3) Ikeda, A.; Shinkai, S. *Chem. Rev.* **1997**, *97*, 1713–1734.
(4) McMahon, G.; O'Malley, S.; Nolan, K. *ARKIVOC* **2003**, *vii*, 23–31.
(5) Alemi, A.A.; Shaabani, B. *Acta Chim. Slov.* **2000**, *47*, 363–369.
(6) Caceres, P.J.; Costamagna, J.; De Namor, A.D.; Matsuhiro, B. *J. Chil. Chem. Soc.* **2004**, *49*, 281–284.
(7) Cho, E.J.; Hwang, S.S.; Oh, J.M.; Kyoung, L.H.; Jeon, S.; Nam, K.C. *Bull. Korean Chem. Soc.* **2001**, *22*, 782–784.
(8) Beer, P.D.; Drew, M.G.B.; Heseka, D.; Nam, K.C. *Chem. Commun.* **1997**, 107–108.
(9) Kim, J.S.; Quang, D.T. *Chem. Rev.* **2007**, *107*, 3780–3799.
(10) Lee, H.D.; Kim, K.H.; Lee, H.J.; Lee, S.; Nanbu, S.; Choe, J.I. *Bull. Korean Chem. Soc.* **2006**, *27*, 508–514.
(11) Macias, A.T.; Norton, J.E.; Evanseck, J.D. *J. Am. Chem. Soc.* **2003**, *125*, 2351–2360.
(12) Konishi, H.; Takahashi, K.; Nakamura, M.; Sakamoto, H.; Kimura, K. *J. Incl. Phenom. Macrocy. Chem.* **2006**, *54*, 147–152.
(13) Talanova, G.G.; Elkarim, N.S.A.; Talanov, V.S.; Bartsch, R.A. *Anal. Chem.* **1999**, *71*, 3106–3109.
(14) Talanova, G.G.; Roper, E.D.; Buie, N.M.; Gorbunova, M.G.; Bartsch, R.A.; Talanov, V.S. *Chem. Commun.* **2005**, 5673–5675.
(15) Ocak, Ü.; Ocak, M.; Surowiec, K.; Bartsch, R.A.; Gorbunova, M.G.; Tu, C.; Surowiec, M.A. *J. Incl. Phenom. Macrocy. Chem.* **2009**, *63*, 131–139.
(16) Ocak, Ü.; Ocak, M.; Shen, X.; Surowiec, K.; Bartsch, R.A. *J. Fluoresc.* **2009**, *19*, 997–1008.
(17) Ocak, Ü.; Ocak, M.; Surowiec, K.; Liu, X.; Bartsch, R.A. *Tetrahedron* **2009**, *65*, 7038–7047.
(18) Ocak, Ü.; Ocak, M.; Shen, X.; Surowiec, K.; Bartsch, R.A. *ARKIVOC* **2010**, *vii*, 81–97.
(19) Tu, C.; Surowiec, K.; Bartsch, R.A. *Tetrahedron Lett.* **2006**, *47*, 3443–3446.
(20) Tu, C.; Liu, D.; Surowiec, K.; Purkiss, D.W.; Bartsch, R.A. *Org. Biomol. Chem.* **2006**, *4*, 2938–2944.
(21) Tu, C.; Surowiec, K.; Bartsch, R.A. *Tetrahedron* **2007**, *63*, 4184–4189.
(22) Tu, C.; Surowiec, K.; Gega, J.; Purkiss, D.W.; Bartsch, R.A. *Tetrahedron* **2008**, *64*, 1187–1196.
(23) Bourson, J.; Valeur, B. *J. Phys. Chem.* **1989**, *93*, 3871–3876.
(24) Desilets, D.J.; Kissinger, P.T.; Lytle, F.E. *Anal. Chem.* **1987**, *59*, 1244–1246.
(25) Lakowicz, J.R. *Principles of Fluorescence Spectroscopy*; Springer: Dordrecht, 2006.